Drug Design, Development and Therapy

Dovepress
Taylor & Francis Group

Open Access Full Text Article

ORIGINAL RESEARCH

D-Mannose Attenuates Ethanol-Induced Gastric Ulcers via Antioxidant Activity Through the HSP90/Nrf2/HO-1 Pathway

Fengzhe Yan[1,*], Xue Yan[2,3,*], Xuefen Li[2,3], Mengya Liu[2], Bing Song[2,3], Ruiyao Zhang[2,3], Yongqiang Duan[1], Yanying Zhang[2,3], Min Bai[1]

[1]School of Traditional Chinese Medicine, Ningxia Medical University, Yinchuan, Ningxia, People's Republic of China; [2]First School of Clinical Medicine, Gansu University of Chinese Medicine, Lanzhou, Gansu, People's Republic of China; [3]Technology Center of Laboratory Animal Industry, Lanzhou, Gansu, People's Republic of China

*These authors contributed equally to this work

Correspondence: Min Bai, School of Traditional Chinese Medicine, Ningxia Medical University, Yinchuan, Ningxia, People's Republic of China, Email 1115487589@qq.com; Yanying Zhang, First School of Clinical Medicine, Gansu University of Chinese Medicine, Lanzhou, Gansu, People's Republic of China, Email zyy@gszy.edu.cn

Purpose: Gastric ulcer (GU) is a prevalent digestive system disease, yet effective treatment methods remain limited. D-mannose, a monosaccharide isolated from Bletilla striata polysaccharides, has been demonstrated to exhibit significant antioxidant potential in previous studies. Prior investigations have not addressed the therapeutic implications of this compound in preventing alcohol-induced gastric epithelial disruptions. This scientific inquiry is designed to investigate the gastroprotective attributes and antioxidant activity of D-mannose in mitigating alcohol-related gastric ulceration.

Methods: An ethanol-induced GU mouse model was established using absolute ethanol. The protective effects and antioxidant activity of different doses of D-mannose (40%, 20% w/v) on gastric tissues were evaluated through morphological observation, pathological staining, and biochemical analysis. Complementarily, computational methodologies encompassing network pharmacological analysis and molecular interaction modeling were utilized to anticipate potential therapeutic mechanisms of D-mannose in gastric ulcer management, subsequently validated through comprehensive experimental investigations in biological systems.

Results: D-mannose significantly reduced the ulcer index and pathological scores in gastric tissues, alleviating the damage induced by absolute ethanol. D-mannose markedly increased the activity of antioxidant enzymes, including superoxide dismutase (SOD), glutathione peroxidase (GSH-Px), and catalase (CAT), while reducing the production of reactive oxygen species (ROS) and malondialdehyde (MDA), thereby enhancing the antioxidant capacity of gastric tissues. Bioinformatics predictions identified HSP90 as the key target for the therapeutic effect of D-mannose on GU. Molecular biology experiments confirmed that D-mannose significantly activated the expression of HSP90 and the downstream Nrf2/HO-1 pathway-related genes and proteins. Similarly, in vitro experiments demonstrated that D-mannose activated key genes and proteins in the HSP90/Nrf2/HO-1 pathway, counteracting oxidative stress damage to gastric epithelial cells induced by absolute ethanol.

Conclusion: D-mannose enhances the antioxidant capacity of gastric tissues by activating key molecules in the HSP90/Nrf2/HO-1 pathway, thereby exerting a protective effect on the stomach.

Keywords: D-mannose, gastric ulcer, oxidative damage, gastroprotective effect, antioxidant activity

Introduction

Gastric ulcer (GU) refers to necrotic defects in the gastric wall that penetrate the entire mucosa and even the muscularis mucosae.[1] Comprehensive epidemiological assessments have revealed gastric ulceration as a critical and widespread gastrointestinal affliction among human populations, affects approximately 10% of the global population, imposing a significant health burden on society.[2] The occurrence of GU is typically attributed to factors such as *Helicobacter Pylori* infection, prolonged use of

Received: 27 April 2025
Accepted: 30 October 2025
Published: 11 December 2025

Graphical Abstract

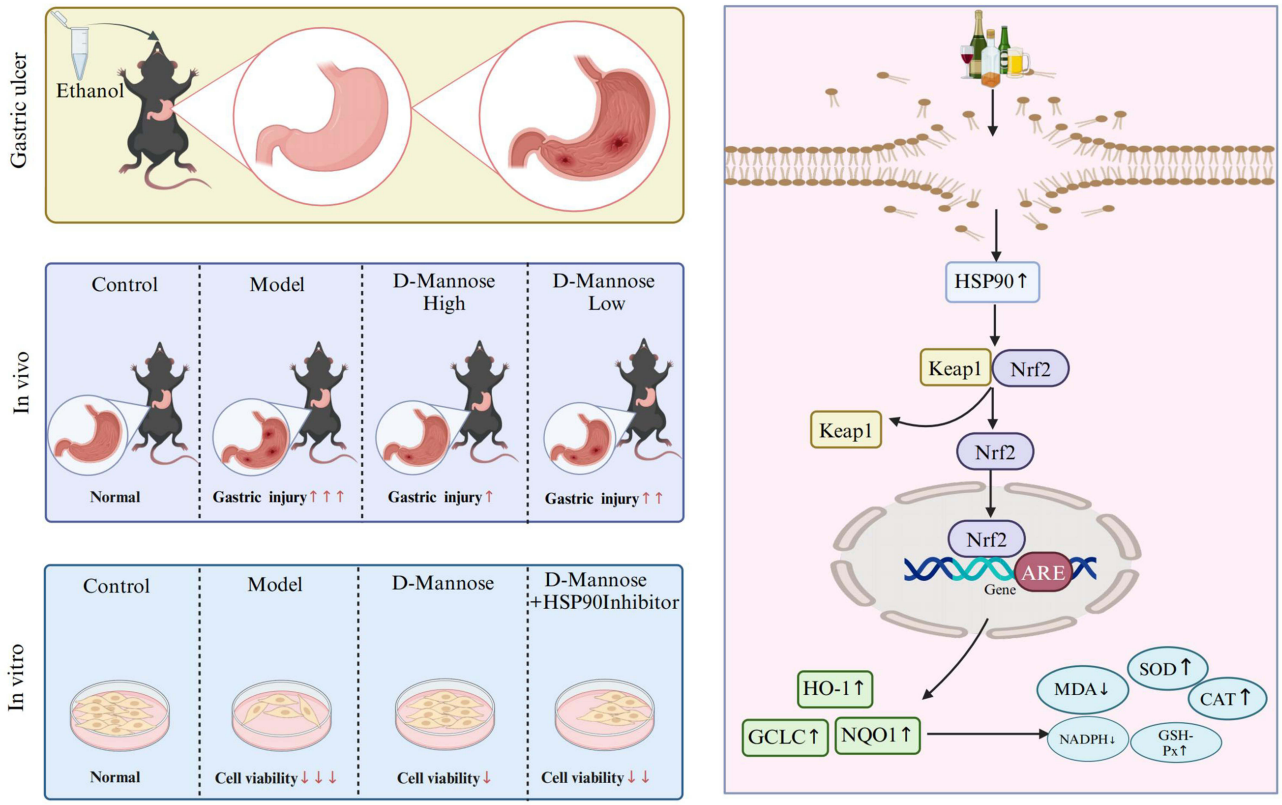

non-steroidal anti-inflammatory drugs (NSAIDs), excessive alcohol consumption, smoking, severe stress, poor dietary habits, or emotional stress and anxiety.[3] Clinically, GU primarily manifests as recurrent, periodic upper abdominal pain, often exacerbated after meals, and is frequently accompanied by nonspecific symptoms such as abdominal distension, nausea, vomiting, reduced appetite, and weight loss. Insufficient and untimely medical treatment of gastric ulceration potentially triggers profound physiological consequences, such as hemorrhagic manifestations, epithelial barrier rupture, pyloric stenosis, and malignant transformation, significantly reducing quality of life and even threatening life safety.[4] Currently, the clinical treatment of GU relies on chemically synthesized drugs, including proton pump inhibitors, H2 receptor antagonists, and gastric mucosal protectants. While these drugs exhibit remarkable therapeutic efficacy, their long-term use can result in adverse effects on the digestive, nervous, cardiovascular, and immune systems.[5] In light of these challenges, systematic investigation of bioactive natural substances with protective gastrointestinal properties becomes increasingly essential.

D-mannose, as a monosaccharide widely distributed in nature, is not only an important component of many plant polysaccharides but also widely present in the body fluids and tissues of animals. A large number of studies have revealed the abundant biological effects of D-mannose, including regulating glucose metabolism, regulating immune responses, and anti-infection, etc.[6] In recent years, with the continuous deepening of research on D-mannose, its potential in antioxidant and anti-inflammatory aspects has gradually emerged. The research by Zhou et al found that during the process of chondrocyte degeneration in osteoarthritis, D-mannose can effectively alleviate oxidative damage of chondrocytes by reducing the excessive accumulation of reactive oxygen species (ROS) and malondialdehyde (MDA), while enhancing the activity of superoxide dismutase (SOD) and glutathione (GSH).[7] Modern pharmacological studies have shown that D-mannose is the main active component of Bletilla striata polysaccharide, and the efficacy of Bletilla striata polysaccharide in treating gastric ulcers has been confirmed.[8] At the same time, Jian et al also found that D-mannose can improve the histopathological damage

of colonic mucosa, thereby alleviating the progression of ulcerative colitis.[9] Based on the above research results, we have reason to speculate that D-mannose may play an important role in ulcerative diseases of gastric tissues.

Oxidative stress refers to an imbalanced state where the excessive production of oxidants surpasses the antioxidant capacity of the cellular defense system. It has been reported that oxidative stress plays a critical role in the development and progression of ethanol-induced GU.[10] Previous studies have indicated that the Nrf2 signaling pathway plays a key role in protecting cells from oxidative damage by activating endogenous antioxidant enzymes.[11] Under normal physiological conditions, Nrf2 remains inactive in the cytoplasm by binding to its negative regulator, Keap1. Upon oxidative stress, Nrf2 dissociates from Keap1, facilitating its translocation from the cytoplasm to the nucleus, leading to the transcriptional activation of Phase II enzyme genes. Among these enzymes, HO-1 is one of the most notably associated with gastrointestinal protection, providing cytoprotection against oxidative stress and preventing apoptosis either directly or through the inhibition of ROS. Current research demonstrates that gallic acid, ethanol extract of sumac fruit, and KFXY can activate the Nrf2/HO-1 signaling pathway, significantly reduce oxidative stress levels, alleviate ethanol-induced gastric mucosal injury, and ameliorate gastric ulcer symptoms.[12]

Network pharmacology represents an innovative scientific approach bridging systems biology and network-based analytical methodologies. As a powerful tool for predicting the complex relationships between drugs, targets, and diseases, it has been successfully applied to uncover the active components and mechanisms of traditional Chinese medicine.[13] Molecular docking allows small-molecule drugs to bind to target proteins spatially, elucidating the binding activity between drugs and their targets.[14] In recent years, numerous studies have adopted combined analyses of network pharmacology and molecular docking to elucidate the mechanisms by which traditional Chinese medicine or natural products treat diseases. Examples include the treatment of atherosclerosis with 6-gingerol,[15] the treatment of solar dermatitis with andrographis paniculata,[16] and the treatment of gastric ulcers with amomi fructus.[17] This study similarly employs this approach to analyze the molecular mechanisms by which D-mannose exerts its antioxidant effects in protecting against ulcerative damage in gastric tissues induced by absolute ethanol. Consequently, comprehensive experimental investigations spanning both in vivo and in vitro domains are executed to substantiate these mechanistic hypotheses, ultimately facilitating D-mannose's potential pharmaceutical and therapeutic translation.

Materials and Methods

Materials

D-Mannose (purity ≥98%) was purchased from Shanghai Macklin Biochemical Co., Ltd. (Shanghai, China). Absolute ethanol was purchased from Tianjin Fuyu Fine Chemical Co., Ltd. (Tianjin, China). Luminespib (HSP90 inhibitor) was obtained from MCE (Shanghai, China), DMEM was sourced from XP Biomed (Shanghai, China), FBS was purchased from Yeasen Biotechnology (Shanghai) Co., Ltd. (Shanghai, China), 0.25% trypsin was purchased from AccuRef Scientific (Xian, China). Penicillin-streptomycin solution and PBS were obtained from Wuhan Servicebio Technology Co., Ltd. (Wuhan, China). The CCK-8 assay kit was purchased from Life-iLab (Shanghai, China). HE staining kits and AB-PAS staining kits were acquired from Wuhan Servicebio Technology Co., Ltd. (Wuhan, China). The ROS fluorescent probe DHE was purchased from Beijing Solarbio Science & Technology Co., Ltd. (Beijing, China). ROS staining solution was obtained from Sigma-Aldrich (Shanghai) Trading Co., Ltd. (Shanghai, China). MDA, SOD, and NADPH assay kits were sourced from LEDA QIBO (#LDQB-E-1090, #LDQB-E-1101, #LDQB-E-1133), GSH-Px and CAT assay kits were procured from Nanjing Jiancheng Bioengineering Institute (A005-1-2, A007-1-1). RNA extraction kits were purchased from Tiangen Biotech (Beijing) Co., Ltd. (DP451). Reverse transcription kits and RT-qPCR amplification kits were obtained from Yeasen Biotechnology (Shanghai) Co., Ltd. (11141ES60, 11201ES50). The HSP90 antibody was sourced from Abcam (AB59459). Nrf2 and HO-1 antibodies were procured from Wuhan Servicebio Technology Co., Ltd. (GB113808, GB11845). The GCLC antibody was purchased from GeneTEX (GTX66057). The NQO1 antibody was purchased from Beijing Biosynthesis Biotechnology Co., Ltd. (BS-2184R).

Animal Experiments

A total of 32 male SPF-grade C57BL/6J mice, aged 2 months and weighing (20 ± 2) g, were obtained from the Experimental Animal Center of Gansu University of Chinese Medicine (Animal Quality Certificate Number: SCXK (Gan) 2021–0001). The

mice were housed in the SPF-grade laboratory of Gansu University of Chinese Medicine (Laboratory Facility Certificate Number: SYXK (Gan) 2021–0004) under controlled conditions: a temperature of 21–25°C, relative humidity of 45–55%, and a 12-hour light/dark cycle. Experimental mice were maintained under ad libitum feeding and hydration conditions. This study strictly adhered to the requirements of the Chinese National Standard "Guidelines for the Welfare and Ethical Review of Laboratory Animals" (GB/T 35892–2018), and all animal experimental protocols were approved by the Animal Welfare and Ethics Committee of Gansu University of Chinese Medicine (Approval Number: 2023–561).

Following a standard one-week acclimatization period, the 32 laboratory mice were randomly assigned to four experimental groups using a random number table: a Control group, a Model group, a D-mannose High-dose group, and a D-mannose Low-dose group, with 8 mice in each group.[18] Control and Model groups received isovolumetric distilled water administration through intragastric gavage. The high- and low-dose D-mannose groups received 0.2 mL of 40% and 20% (w/v) D-mannose, respectively, via gavage.[19] All groups were treated for 7 consecutive days.[20] At the 24-hour mark subsequent to the terminal dosing, the reference group underwent oral gavage administration of matched distilled water volume, while the remaining groups were given 10 mL/kg of absolute ethanol via gavage to induce ulcerative damage in gastric tissues.[21] Food was withheld for 24 hours prior to ethanol administration, but water was provided ad libitum. Two hours after ethanol gavage, the mice in each group were anesthetized with isoflurane inhalation. The peritoneal space was accessed to retrieve the complete gastric organ, subsequently bisected along its major anatomical arc and meticulously cleansed using isotonic saline solution. Photographs were taken of the cleaned gastric tissues. Selected tissue fragments were immobilized in 4% formalin for pathological examination and histological visualization, concurrently, the alternate tissue segments were instantaneously frozen and archived in a cryogenic repository maintained at −80°C, earmarked for advanced molecular research protocols. The specific experimental procedure is shown in Figure 1.

Cell Culture

Human gastric mucosal epithelial cells (GES-1) were purchased from FuHeng BioLogy, product no. FH0273. The culture medium for GES-1 cells was complete DMEM medium containing 10% fetal bovine serum (FBS) and 1% penicillin-streptomycin mixture. The culture flasks were placed in an incubator maintained at 37°C with 5% CO_2 for cultivation.

GES-1 cells in the logarithmic growth phase (1×10^5 cells/mL) were seeded at 150 μL per well into 96-well culture plates and cultured for 24 hours. Cells were treated with D-mannose at concentrations of 5, 10, 20, 40, 80, 160, and 320 mg/mL for 24 and 48 hours. The cytotoxicity of D-mannose on GES-1 cells was assessed using the CCK-8 assay. Additionally, cells were exposed to absolute ethanol at concentrations of 0.2, 0.4, 0.6, 0.8, 1.0, and 1.2 mol/L for 2, 6, and 12 hours. Cell viability was measured using the CCK-8 assay, while MDA content in GES-1 cells was determined by

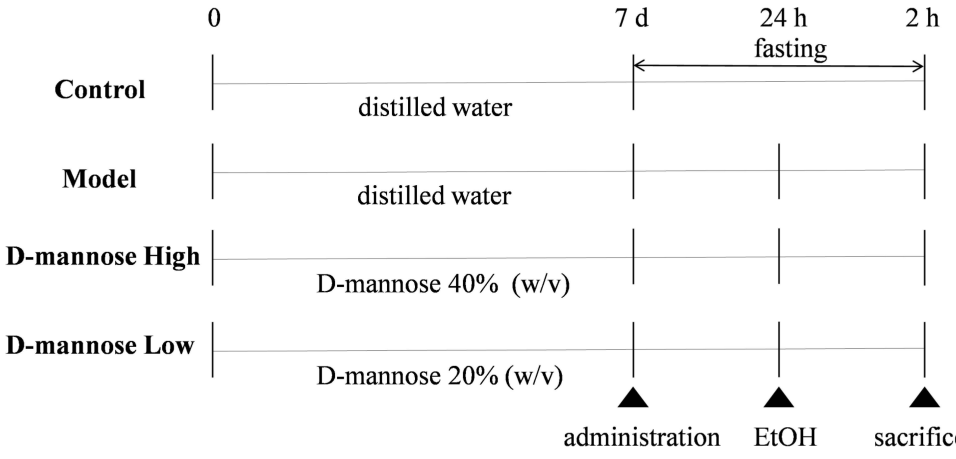

Figure 1 Architectural blueprint depicting the investigative approach for creating a mouse model of alcohol-induced gastric tissue disruption. D-mannose was administered continuously for 7 days. Twenty-four hours after the final administration, ethanol was used to induce ulcerative damage in gastric tissues. Tissue collection was performed 2 hours after ethanol stimulation under anesthesia.

biochemical methods. These experiments were conducted to comprehensively evaluate the optimal concentration and exposure time for ethanol-induced damage.

Macroscopic Observation of Gastric Tissues

The gastric tissue damage in mice from each group was observed. The ulcer index was analyzed using Image J software. The formula for calculating the ulcer index is as follows: Ulcer Index (percentage of mucosal area affected) = (Gastric Damage Area / Gastric Mucosal Area) × 100%.[22]

Histopathological Observation of Gastric Tissues

After fixation of the gastric tissues, the samples were subjected to ethanol gradient dehydration, paraffin embedding, and sectioning using a microtome. Hematoxylin and eosin (HE) staining and Alcian Blue-Periodic Acid-Schiff (AB-PAS) staining were performed. Microscopic examination revealed distinctive morphological alterations and architectural modifications within the gastric mucosal specimens derived from each experimental cohort. The gastric tissue was evaluated based on four pathological criteria: epithelial cell loss (scored 0–3), mucosal edema (scored 0–4), hemorrhagic lesions (scored 0–4), and inflammatory cell infiltration (scored 0–3), with a maximum total score of 14 points.[23] For AB-PAS staining, the mucus coverage of the gastric mucosa in mice from each group was observed under a microscope. The mucus-associated surface region of gastric mucosal tissues underwent precise digital quantification through specialized Image J analytical algorithms. All the aforementioned result evaluations, including ulcer index, histopathological analysis, and mucus area, were performed by researchers who were blinded to the treatment groups.

Morphological Observation of Gastric Tissues Under Electron Microscopy

Fresh gastric tissue was cut into small blocks (1mm^3) and rinsed with pre-cooled PBS to remove gastric contents. Subsequently, the samples were placed in electron microscope fixation solution and fixed at room temperature for 2 hours. After PBS washing, the samples were transferred to 1% osmium acid solution and fixed in the dark for 1–2 hours. Preservation-stabilized samples were systematically dehydrated through a graduated ethanol series and subsequent isopentyl acetate processing. Finally, the samples were dried using a critical point drying apparatus, adhered to conductive carbon film double-sided tape, and subjected to gold sputtering using an ion sputter coater. The specimens were then observed and imaged using a scanning electron microscope.

Determination of ROS Content in Gastric Tissue (Cells)

Gastric Tissue: Due to the specificity of ROS detection, frozen sections of gastric tissue were prepared. ROS dye was then applied to the sections, followed by counterstaining of nuclei with DAPI. After slight drying of the sections, an antifluorescence quenching sealing reagent was used to seal the slides. Microscopic visualization of the sections was conducted using fluorescence optical technology, with comprehensive image documentation. The average OD of the images was analyzed using Image J software, and semi-quantitative analysis was performed.

GES-1 Cells: The oxidative cellular environment of GES-1 cells was comprehensively analyzed through DHE fluorescence detection, implementing the precise methodological instructions provided by the specialized ROS probe kit manufacturer. As a premier cell-penetrating fluorescent probe, DHE has emerged as a gold standard technique for quantifying intracellular oxidative dynamics within living cellular environments. DHE itself exhibits blue fluorescence. After entering live cells, it is dehydrogenated under the action of ROS, leading to the oxidation product Ethidium. Ethidium binds to DNA, producing red fluorescence. Researchers prepared the DHE solution by diluting the probe to a 10 μM concentration using comprehensive culture medium, subsequently maintaining the sample in darkness at room temperature for a precise 30-minute interval. Following the specified incubation period, cellular specimens underwent systematic cleansing using PBS. Through specialized fluorescence microscopy techniques, the cellular fluorescent characteristics were meticulously observed and photographically captured. Employing Image J analytical software, researchers conducted semi-quantitative evaluation by measuring the mean OD of the acquired microscopic images.

Determination of Oxidative Stress-Related Molecules in Gastric Tissue (Cells)

A rigorous homogenization approach was applied to gastric tissue and GES-1 cellular systems, involving disruption in pre-chilled phosphate-buffered saline adjusted to a pH of 7.4. Utilizing controlled centrifugation parameters, the sample was processed at 4°C, spinning at 4000 r/min for 20 minutes, followed by systematic supernatant collection. In strict adherence to the protocol specified by the respective assay kits, we quantified the concentrations of molecules associated with oxidative stress, including SOD, GSH-Px, CAT, MDA, and NADPH, were measured in the gastric tissue and GES-1 cells.

Bioinformatics Analysis

Network Pharmacology

The 3D chemical structure of D-mannose was retrieved from the PubChem database and saved in sdf format file. The file was then uploaded to the SwissTarget database to predict its target molecules. Meanwhile, the GeneCards database was used to identify disease-related target molecules for "gastric ulcer". The intersection of the two sets of target molecules was identified as the key molecules for D-mannose in the treatment of gastric ulcers. Subsequently, PPI analysis was performed on the intersecting targets using the String database. The resulting TSV format file was imported into Cytoscape 3.8.0 software for topological parameter analysis. Secondary screening of the obtained genes was conducted using the criterion that all of the following parameters—Betweenness, Closeness, Degree, Degree Layout, Eigenvector, Information, LAC, and Network—must exceed their respective median values. Ultimately, key targets were identified through this process.

Molecular Docking

The 3D chemical structure of D-mannose was retrieved from the PubChem database and saved in sdf format. The key target receptors predicted by network pharmacology were downloaded from the PDB database and saved as PDB format files. Using DS BIOVIA Discovery Studio Client 2019 software, molecular docking was performed between the D-mannose small molecule ligand and the key target receptors. The results were exported and analyzed.

Determination of Gene Expression Related to the HSP90/Nrf2/HO-1 Pathway in Gastric Tissue (Cells)

Reverse transcription quantitative polymerase chain reaction(RT-qPCR) was used to detect the mRNA expression levels of *HSP90, Nrf2, HO-1, NQO1, GCLC* in gastric tissue (GES-1 cells). Total RNA was routinely extracted from gastric tissue (GES-1 cells) using a total RNA extraction kit for animal tissues/cells, and the RNA concentration was measured. The A260/A280 ratio was maintained within the range of 1.8–2.0. A reverse transcription kit was used to prepare a 20 μL system to reverse-transcribe RNA into cDNA for subsequent PCR amplification reactions. For precision in genetic quantification, *β-Actin* was selected as the endogenous control gene, and an amplification kit was used for RT-qPCR amplification to obtain the Ct values for each amplification reaction. Relative messenger RNA expression levels were precisely assessed via the standardized $2^{-\Delta\Delta Ct}$ analytical technique. The sequences of the primers used are shown in Table 1.

Determination of Protein Expression Related to the HSP90/Nrf2/HO-1 Pathway in Gastric Tissue (Cells)

Western Blot (WB) Analysis

Protein expression was comprehensively examined via the Western blotting technique for HSP90, Nrf2, HO-1, NQO1, and GCLC in gastric tissue (GES-1 cells). Protein extraction from GES-1 cells was performed through RIPA buffer treatment, with protein concentration subsequently measured via BCA assay kit protocols. After denaturation of the proteins in a 100°C metal bath, equal amounts of protein (30 μg per sample) were loaded onto SDS-PAGE gels for electrophoresis separation. Protein isolates underwent electroblotting, facilitating their migration and immobilization onto PVDF membrane substrates. The membrane was immersed in a rapid protein-free blocking solution for 15 minutes to block nonspecific binding, followed by washing with TBST. Subsequently, rabbit polyclonal antibodies against

Table 1 Primers Sequences for RT-qPCR

Gene	Forward Primer (5′~3′)	Reverse Primer (5′~3′)
HSP90(M)	AAGGATGTACAGATGCTGCAAGAC	AGAGGCCAGAATCGATGCAA
HSP90(H)	CAGTACGCTTGGGAGTCCTCA	TTTGTTCCACGACCCATAGGTTC
Nrf2(M)	TCAGCATGATGGACTTGGAGTTG	ACTTGTACCGCCTCGTCTGGA
Nrf2(H)	TGGGCCCATTGATGTTTCTG	TGCCACACTGGGACTTGTGTTTA
HO-1(M)	TCACTTCGTCAGAGGCCTGCTA	AGCGGTGTCTGGGATGAGCTA
HO-1(H)	GCCAGCAACAAAGTGCAAGA	AGTGTAAGGACCCATCGGAGAA
NQO1(M)	AGGACGCCTGAGCCCAGATA	AGGCAAATCCTGCTACGAGCAC
NQO1(H)	CTTCTGGAAGTCATCTCATTCCAC	TTTCCAGCTCGGTCCAATC
GCLC(M)	GCACATCTACCACGCAGTCAA	CATGATCGAAGGACACCAACA
GCLC(H)	CAAGGGTAATCTTGGGTTTCTAGCA	CCTTTGATAACAGCCATCAGAGTTC
β-Actin(M)	CATCCGTAAAGACCTCTATGCCAAC	ATGGAGCCACCGATCCACA
β-Actin(H)	TGGCACCCAGCACAATGAA	CTAAGTCATAGTCCGCCTAGAAGCA

Abbreviations: AB-PAS, alcian blue-periodic acid-schiff; CAT, catalase; CCK-8, cell counting kit-8; DMEM, dulbecco's modified eagle medium; FBS, fetal bovine serum; GU, gastric ulcer; GES-1, human gastric mucosal epithelial cells; GSH, glutathione; GSH-Px, glutathione peroxidase; GCLC, glutamate cysteine ligase catalytic subunit; HE, hematoxylin and eosin; HSP90, heat shock protein 90; HO-1, heme oxygenase-1; MDA, malondialdehyde; NADPH, nicotinamide adenine dinucleotide phosphate; Nrf2, nuclear factor erythroid 2-related factor 2; NQO1, NAD (P) H quinone oxidoreductase 1; ROS, reactive oxygen species; RT-qPCR, reverse transcription quantitative polymerase chain reaction; SOD, superoxide dismutase; WB, western blot.

HSP90, Nrf2, HO-1, GCLC, and NQO1 were added at a specified dilution ratio, and the membrane was incubated overnight at 4°C. After initial processing, the membrane was systematically rinsed with TBST solution, whereupon an HRP-conjugated goat anti-rabbit IgG antibody, prepared at a 1:5000 concentration, was introduced and allowed to interact at standard laboratory temperature for a 60-minute interval. Post extensive TBST washing, the membrane was subjected to ECL reagent application, enabling protein band visualization through advanced imaging instrumentation. The luminescent protein bands underwent density measurement and systematic interpretation via Image J analytical platform.

Immunofluorescence

Immunofluorescence was employed to detect the protein expression levels of HSP90, Nrf2, HO-1, NQO1, and GCLC in gastric tissue. Prepared paraffin sections were used to determine the expression of the related proteins, and the corresponding antibodies were applied to the paraffin sections. Finally, the nuclei were counterstained with DAPI. After air-drying the sections slightly, they were sealed with an anti-fluorescence quenching mounting medium. The tissue sections were subjected to detailed fluorescence-based optical analysis, followed by precise image capturing procedures. The average OD of the images was analyzed using Image J, and semi-quantitative analysis was performed.

Statistical Analysis

First, the Shapiro–Wilk test was used to determine whether the experimental data conformed to a normal distribution. If the data conformed to a normal distribution, it was expressed as the mean ± standard deviation; if not, the median and interquartile range were used. For normally distributed data, one-way analysis of variance (ANOVA) was used for intergroup comparison. If the result was significant ($P < 0.05$), post hoc tests were conducted (LSD was used when variances were homogeneous, and Tamhane's T2 was used when variances were heterogeneous). For non-normally distributed data with a small sample size ($n < 5$), permutation tests were used. $P < 0.05$ indicated a statistically significant difference between groups.

Results

D-Mannose Improves Gross Morphological and Pathological Features of Ethanol-Induced Gastric Ulcers in Mice

To investigate the therapeutic effect of D-mannose on ethanol-induced GU, mice were pretreated with different doses of D-mannose (40% and 20% w/v) for one week, followed by the induction of gastric ulcerative damage using absolute ethanol. First, the morphological changes in the gastric tissue of each group of mice were observed macroscopically. As depicted in Figure 2A, the Model group presented marked hemorrhagic alterations, displaying extensive linear and punctate lesional signatures, which definitively indicated the precise creation of the gastric ulcer investigative model. However, mice in the D-mannose administration resulted in a marked attenuation of hemorrhagic lesion severity. Subsequently, the ulcer area in gastric tissue was quantitatively analyzed using Image J software. The statistical results were consistent with the morphological observations. Ulcer index reached peak levels in the Model group, while D-mannose intervention groups exhibited markedly diminished lesional severity compared to the Model cohort ($P < 0.05$), as documented in Figure 2B. We conducted HE staining to provide in-depth microscopic insights into the pathological transformations of gastric tissue. When juxtaposed

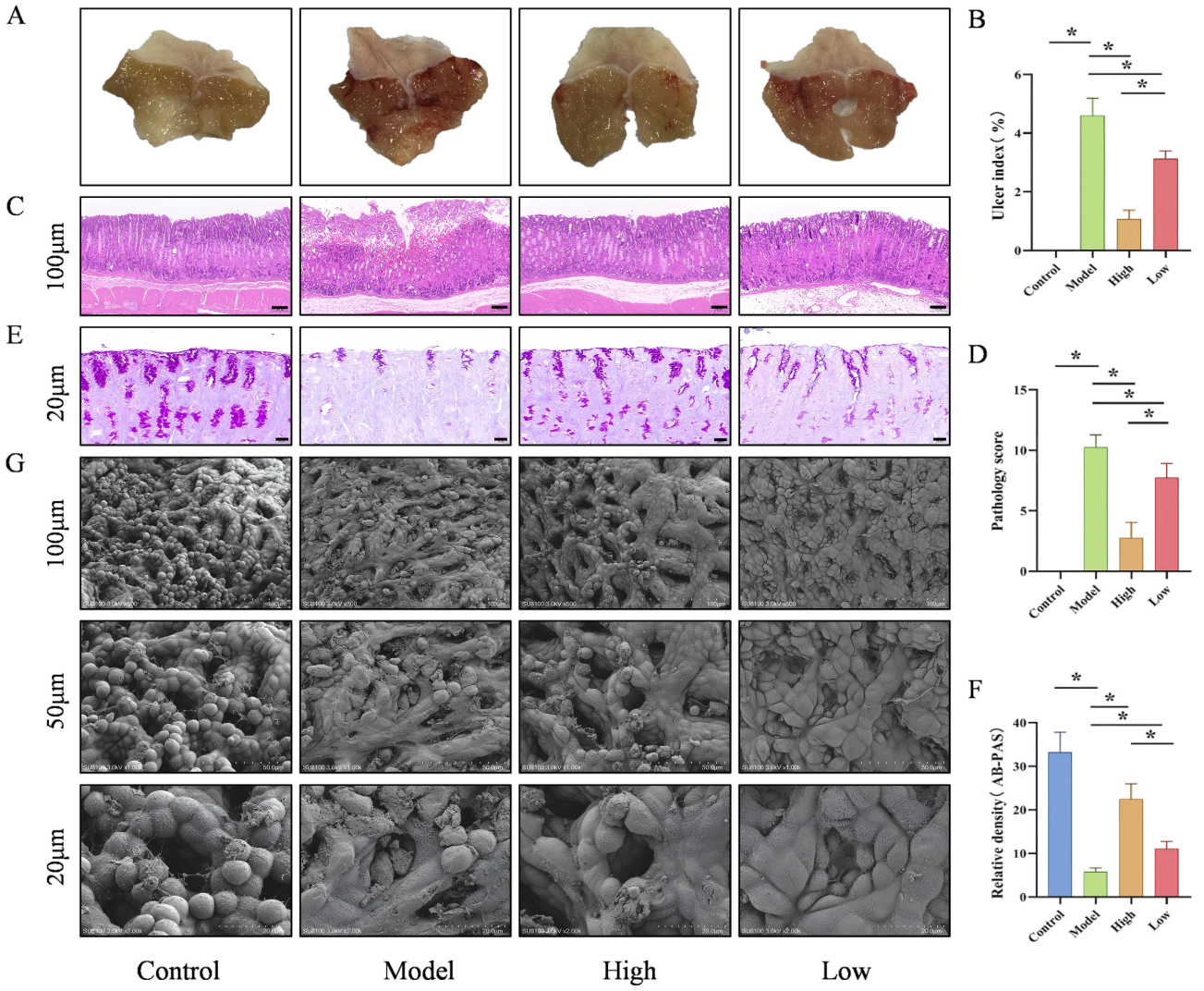

Figure 2 D-Mannose Improves Gross Morphological and Pathological Features in Ethanol-Induced GU Mice. (**A**) Macroscopic images of gastric tissue (n=8); (**B**) Ulcer index (n=8); (**C**) Representative HE-stained images (100 μm; n=8); (**D**) Pathological scores (n=8); (**E**) Representative AB-PAS-stained images (20 μm; n=8); (**F**) Mucin Coverage Analytical Evaluation (n=8); (**G**) Representative SEM images (100 μm, 50 μm, 20 μm; n=3). Data are presented as mean±SD and were analyzed by one-way ANOVA followed by LSD/Tamhane's T2 post hoc test. *means $P < 0.05$.

with the Control group, the Model group mice displayed marked epithelial cell reduction, disrupted gastric gland architecture, hemorrhagic damage, and infiltration of inflammatory cells, along with significantly elevated pathological scores, as evidenced in Figure 2C and D. In contrast, these injuries were markedly alleviated in the D-mannose-treated groups, with improved pathological scores. Additionally, we employed AB-PAS staining to evaluate mucin secretion in the gastric tissue of each group, which reflects the functionality of the gastric tissue's chemical barrier. Evidenced in Figure 2E and F, the Model group demonstrated a substantial decrease in mucosal mucin distribution, achieving statistical significance ($P < 0.05$). Conversely, groups subjected to D-mannose treatment presented a significant upregulation of mucin density across the gastric mucosal interface ($P < 0.05$). In addition, we used scanning electron microscopy to focus on the morphology of gastric epithelial cells and gastric pits. In the Control group, gastric epithelial cells appeared intact, with a clearly visible mucosal surface and well-defined gastric pits. In contrast, the Model group mice, induced by absolute ethanol, exhibited severe damage to gastric epithelial cells and disruption of gastric pit structures. The D-mannose-treated cohorts exhibited a significant morphological restoration of gastric epithelial cellular arrangement and pit organization (Figure 2G). The above results indicate that D-mannose exerts a certain protective effect on absolute ethanol-induced GU in mice, with the high-dose group demonstrating significantly superior intervention efficacy compared to the low-dose group.

D-Mannose Alleviates Oxidative Stress in GU Mice

Oxidative stress represents a pivotal mechanism underlying the pathogenesis of ethanol-mediated GU. Therefore, we assessed oxidative stress-related markers in gastric tissues. Immunofluorescence results demonstrated that, compared to the Control group, the ROS levels in the gastric tissues of the Model group were significantly increased ($P < 0.05$). Interestingly, ROS concentrations in gastric tissues exhibited a significant, dose-correlated diminution following D-mannose treatment ($P < 0.05$; Figure 3A and B). Biochemical assay results showed that, compared to the Control group, the Model group exhibited significantly elevated levels of MDA and NADPH ($P < 0.05$) and significantly decreased activities of the antioxidant enzymes SOD, GSH-Px, and CAT ($P < 0.05$). However, these changes were markedly reversed in the gastric tissues of the D-mannose group ($P < 0.05$; Figure 3C–G). These results demonstrate that D-mannose exerts gastroprotective effects by reducing the generation of ROS, MDA, and NADPH while enhancing the activities of SOD, GSH-Px, and CAT, with the high-dose group showing significantly superior efficacy compared to the low-dose group.

Bioinformatics Prediction of Target Molecules for D-Mannose in GU Treatment

The 3D chemical structure of D-mannose was retrieved from the PubChem database and saved in sdf format. This file was uploaded to the SwissTarget database to predict potential target molecules, resulting in a total of 76 predicted targets. Simultaneously, the Genecards database was queried for "gastric ulcer"-related molecular targets, identifying 6508 disease-related targets. Intersecting these two datasets yielded 51 overlapping genes. PPI network configuration was conducted utilizing the String computational database for the identified intersecting gene sets, followed by topological parameter analysis of the PPI network with Cytoscape software. Four core genes were identified: HSP90AA1, PRKCA, ESR2, and STAT3 (Figure 4A). Subsequently, protein crystal structure files (in PDB format) for the target proteins HSP90AA1 (PDB ID: 7S9H), STAT3 (PDB ID: 6NJS), ESR2 (PDB ID: 7XWQ), and PRKCA (PDB ID: 8U37) were downloaded from the Protein Data Bank (PDB). Molecular docking analyses between D-mannose and the four receptors were performed using DS BIOVIA Discovery Studio Client 2019 software. LibDock computational analysis generated interaction scores, highlighting the molecular binding characteristics of D-mannose with HSP90AA1, STAT3, ESR2, and PRKCA were 84.6236, 82.4886, 69.1632, and 72.3774, respectively (Figure 4B). These findings suggest that D-mannose exhibits the strongest binding affinity to HSP90AA1. Findings demonstrate HSP90AA1 as a key molecular mechanism underlying D-mannose's therapeutic efficacy in gastric ulcer treatment.

D-Mannose Activates the HSP90/Nrf2/HO-1 Signaling Pathway in GU Mice

As a pivotal molecular chaperone, HSP90 interacts genetically and physically with Nrf2, serving a fundamental role in mitigating oxidative damage pathways. Applying state-of-the-art molecular biology strategies, we evaluated the genetic and proteomic expression profiles of HSP90 and essential signaling molecules in the Nrf2/HO-1 pathway within gastric tissues. Quantitative RT-qPCR analysis revealed statistically significant upregulation of *HSP90, Nrf2, HO-1* and *NQO1*

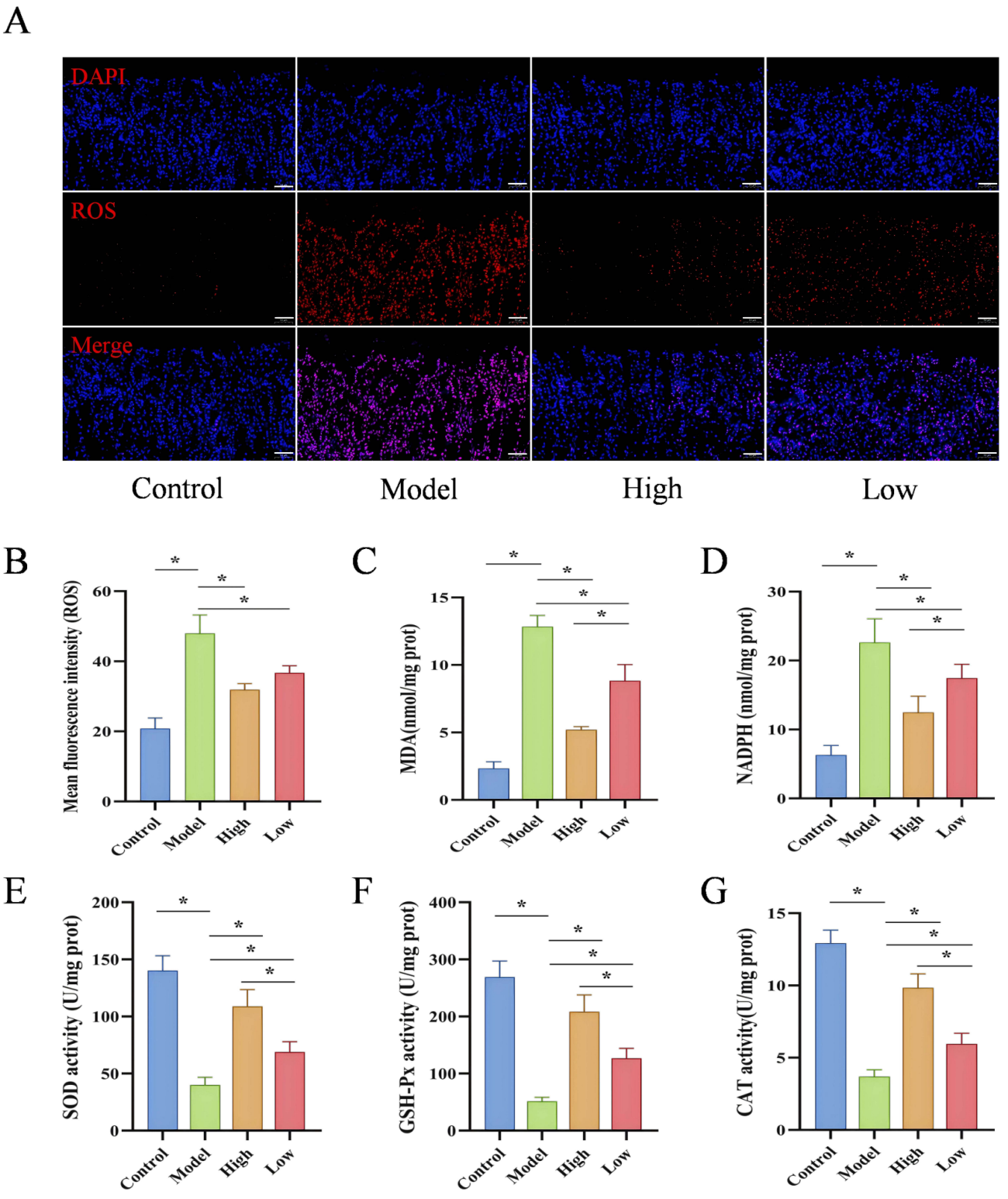

Figure 3 D-Mannose Alleviates Oxidative Stress in GU Mice. (**A** and **B**) Immunofluorescence detection of ROS expression in gastric tissues and quantitative analysis of ROS levels (50 μm, n=3); (**C–G**) Biochemical assay results of MDA, NADPH, SOD, GSH-Px, and CAT levels (n=3). Brightness and contrast adjustments were applied uniformly using Case Viewer 2.4 (**A**). Data are presented as mean±SD and were analyzed by one-way ANOVA followed by LSD/Tamhane's T2 post hoc test. *means $P < 0.05$.

mRNA transcripts in Model group gastric tissues compared to Control specimens ($P < 0.05$). The D-mannose group exhibited markedly higher mRNA expression profiles compared to the Model group, with statistically significant differences ($P < 0.05$), as illustrated in Figure 5A–E. Subsequently, immunofluorescence and WB were used to detect

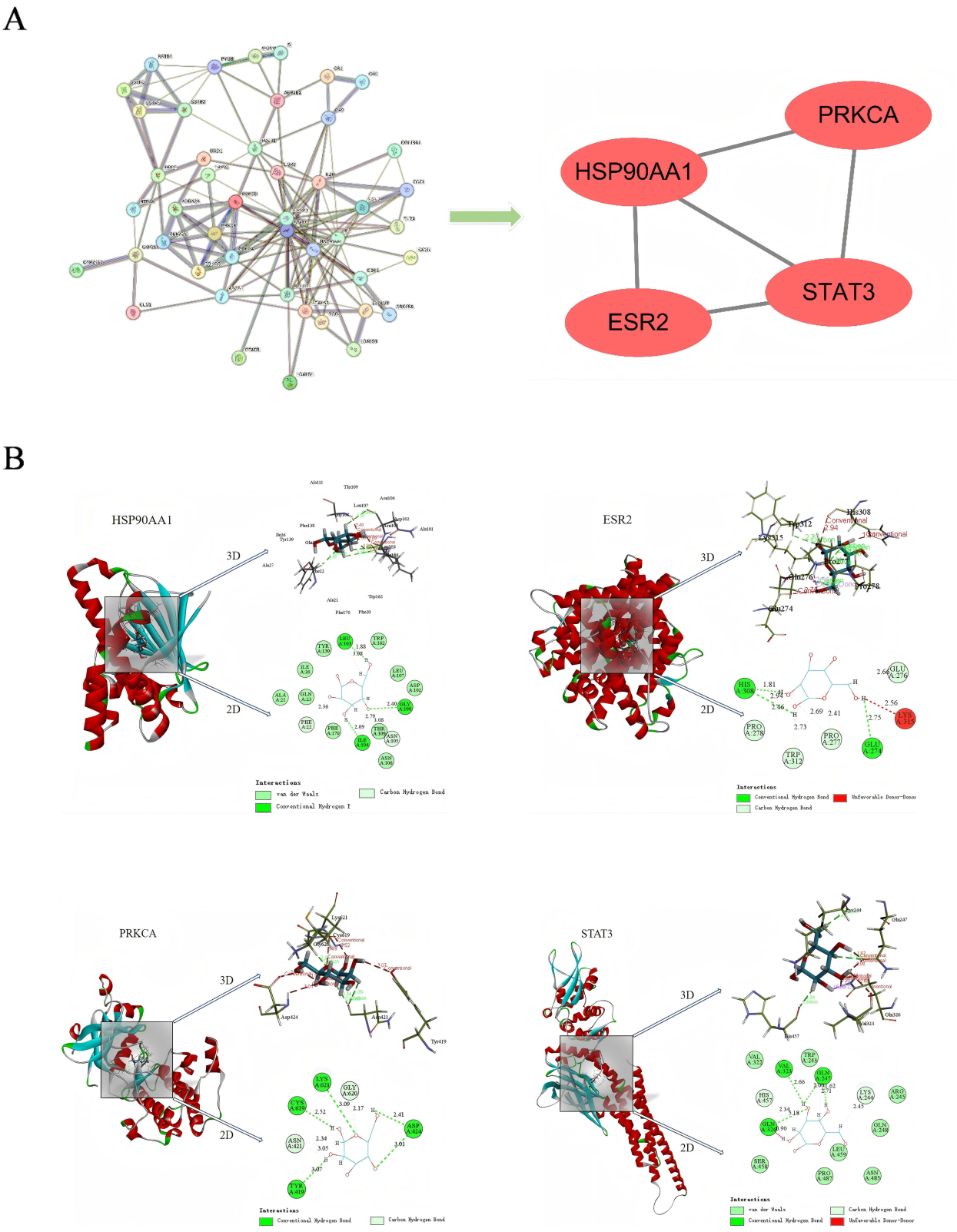

Figure 4 Bioinformatics Prediction of Target Molecules for D-Mannose in GU Treatment. (**A**) PPI network and topological analysis of target molecules; (**B**) Molecular docking results of D-mannose with core target molecules. HSP90AA1: Grid box radius = 8.00 Å, dimensions (22.46, 10.64, −26.25), Libdock score = 84.6236; ESR2: Grid box radius = 8.00 Å, dimensions (7.00, −18.03, −49.40), Libdock score = 69.1632; PRKCA: Grid box radius = 8.00 Å, dimensions (31.74, −12.88, 18.20), Libdock score = 72.3774; STAT3: Grid box radius = 7.00 Å, dimensions (0.70, 14.00, 24.65), Libdock score = 82.4886.

https://doi.org/10.2147/DDDT.S525021

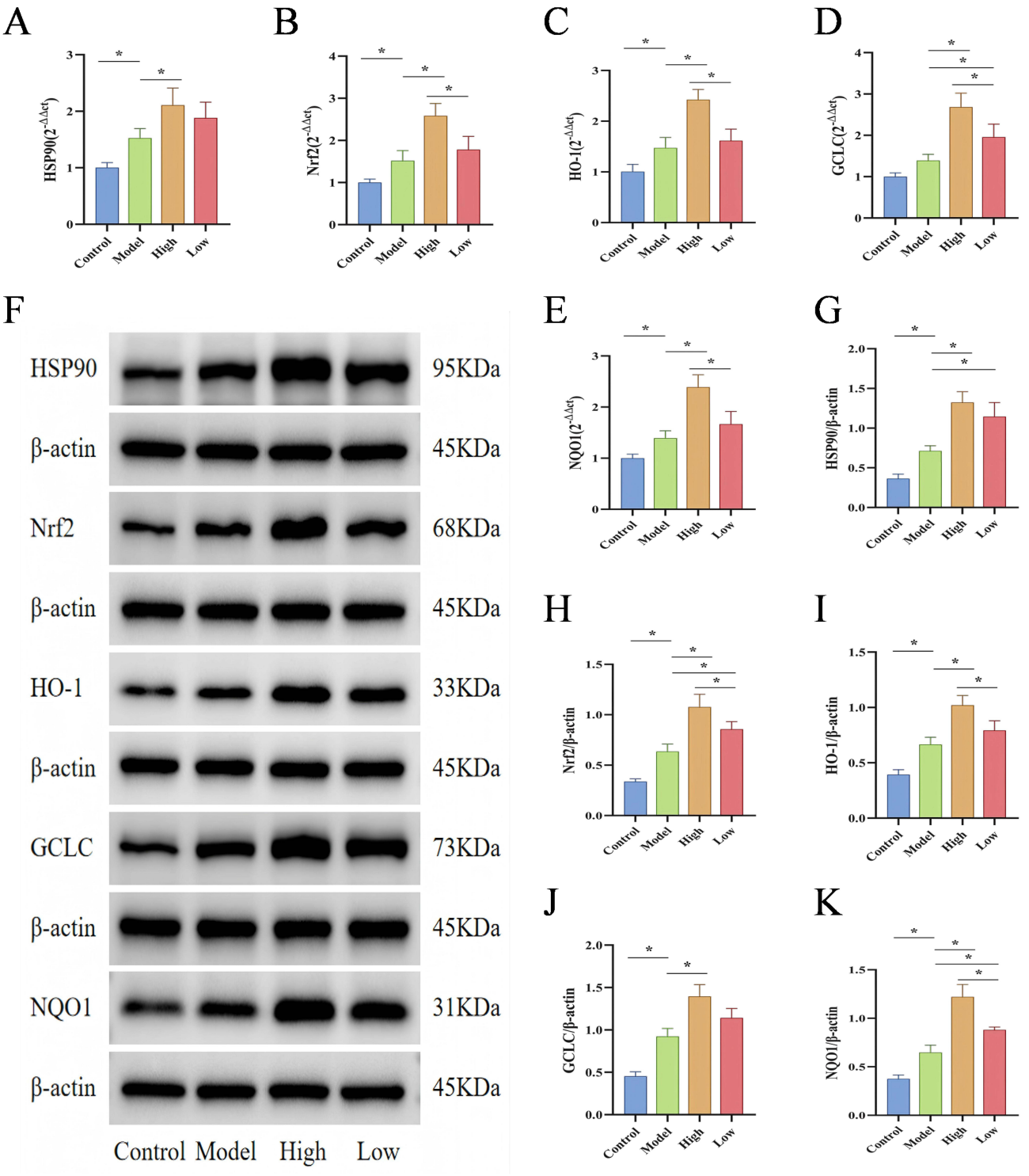

Figure 5 Effects of D-Mannose on the Gene and Protein Expression of Key Molecules in the HSP90/Nrf2/HO-1 Pathway. (**A–E**) RT-qPCR analysis of mRNA levels of *HSP90, Nrf2, HO-1, NQO1,* and *GCLC* in gastric tissues (n=3); (**F–K**) Western blot detection of HSP90, Nrf2, HO-1, NQO1, and GCLC protein expression and quantitative analysis (n=3). Brightness and contrast adjustments were applied uniformly using Image J 1.42q (**F**). Data are presented as mean±SD and were analyzed by one-way ANOVA followed by LSD/Tamhane's T2 post hoc test. *means $P < 0.05$.

protein expression levels, and the results were consistent with those obtained from RT-qPCR. Compared to the Control group, the protein levels of HSP90, Nrf2, HO-1, NQO1, and GCLC in the gastric tissues of the Model group were significantly elevated ($P < 0.05$). The D-mannose group exhibited substantially increased protein expression profiles

when contrasted with the Model group, presenting statistically significant differences ($P < 0.05$), as visualized in Figures 5F–K and 6. The above results indicate that D-mannose enhances the antioxidant capacity of gastric tissue by activating the HSP90/Nrf2/HO-1 signaling pathway, with the high-dose group demonstrating significantly superior intervention effects compared to the low-dose group.

The Interventional Effect of Different Concentrations of D-Mannose on Ethanol-Induced Oxidative Damage in GES-1 Cells

To better elucidate the molecular mechanism of D-mannose in protecting against ethanol-induced gastric tissue injury, we first treated GES-1 cells with 0.2 mol/L, 0.4 mol/L, 0.6 mol/L, 0.8 mol/L, 1.0 mol/L, and 1.2 mol/L absolute ethanol. The results showed that different concentrations of absolute ethanol had no significant effect on cell viability after 2 h. However, the content of MDA in the cells treated with absolute ethanol was significantly increased ($P < 0.05$). Since no significant difference was observed between 1.0 and 1.2 mol/L concentrations, the optimal modeling conditions for absolute ethanol were determined as 1.0 mol/L for 2 hours based on integrated analysis of CCK-8 and biochemical assays (Figure 7A and B). Subsequently, we prepared D-mannose at concentrations of 5 mg/mL, 10 mg/mL, 20 mg/mL, 40 mg/mL, 80 mg/mL, 160 mg/mL, and 320 mg/mL using complete culture medium to treat GES-1 cells. The results demonstrated that 40 mg/mL D-mannose achieved a 40% inhibition rate after 24 hours intervention. Therefore, subsequent experiments employed D-mannose at concentrations of 40, 20, and 10 mg/mL for further investigation (Figure 7C).

We then treated ethanol-induced GES-1 cells with different concentrations of D-mannose (40, 20, and 10 mg/mL). Fluorescence microscopy analysis revealed markedly higher ROS levels in the ethanol-exposed Model group, showing statistically significant elevation relative to the Control group *(*$P < 0.05$). In contrast, pretreatment with D-mannose at varying concentrations led to a dose-dependent decrease in intracellular ROS levels ($P < 0.05$; Figure 8A and B). In addition, the results from biochemical assay showed that, compared with the Control group, the Model group of GES-1 cells exhibited significantly increased levels of MDA and NADPH ($P < 0.05$), while the activities of SOD, GSH-Px, and CAT were significantly decreased ($P < 0.05$). After pretreatment with D-mannose, these parameters were markedly reversed, with the most pronounced effects observed at a concentration of 40 mg/mL ($P < 0.05$; Figure 8C–G). These findings indicate that D-mannose significantly enhances the antioxidant capacity of GES-1 cells, counteracting the oxidative damage induced by absolute ethanol, with the optimal protective effect achieved at a concentration of 40 mg/mL.

D-Mannose Enhances Antioxidant Activity in GES-1 Cells by Activating Key Molecules in the HSP90/Nrf2/HO-1 Pathway

To verify that the HSP90/Nrf2/HO-1 pathway is the key mechanism by which D-mannose mitigates oxidative damage in GES-1 cells, we conducted experiments using the HSP90 inhibitor Luminespib to suppress HSP90 expression. We first examined the mRNA and protein expression levels of key molecules in the HSP90/Nrf2/HO-1 signaling pathway in GES-1 cells. The results showed that, compared with the Control group, treatment with absolute ethanol significantly increased the mRNA and protein levels of *HSP90, Nrf2, HO-1, NQO1* and *GCLC* in the Model group of GES-1 cells ($P < 0.05$). Pretreatment with D-mannose further upregulated the mRNA and protein levels of *HSP90, Nrf2, HO-1, NQO1 and GCLC* compared to the Model group ($P < 0.05$). However, in the D-mannose + Luminespib co-treatment group, the expression of these molecules was significantly downregulated ($P < 0.05$; Figure 9). We then measured oxidative stress-related indicators. Quantitative analysis indicated that ethanol intervention dramatically altered oxidative stress profiles in GES-1 cells, with significant escalation of ROS, MDA, and NADPH levels, alongside pronounced decreases in antioxidant enzyme activities ($P < 0.05$). Molecular evaluation showed that D-mannose pretreatment significantly rebalanced cellular oxidative mechanisms, substantially reducing oxidative stress indicators and boosting protective enzymatic activities ($P < 0.05$). Co-administration of D-mannose with Luminespib counteracted the protective effects, resulting in significant reactivation of oxidative stress markers, characterized by substantial increases in ROS, MDA, and NADPH levels, accompanied by significant reductions in SOD and CAT enzymatic activities ($P < 0.05$; Figure 10). The experimental findings conclusively

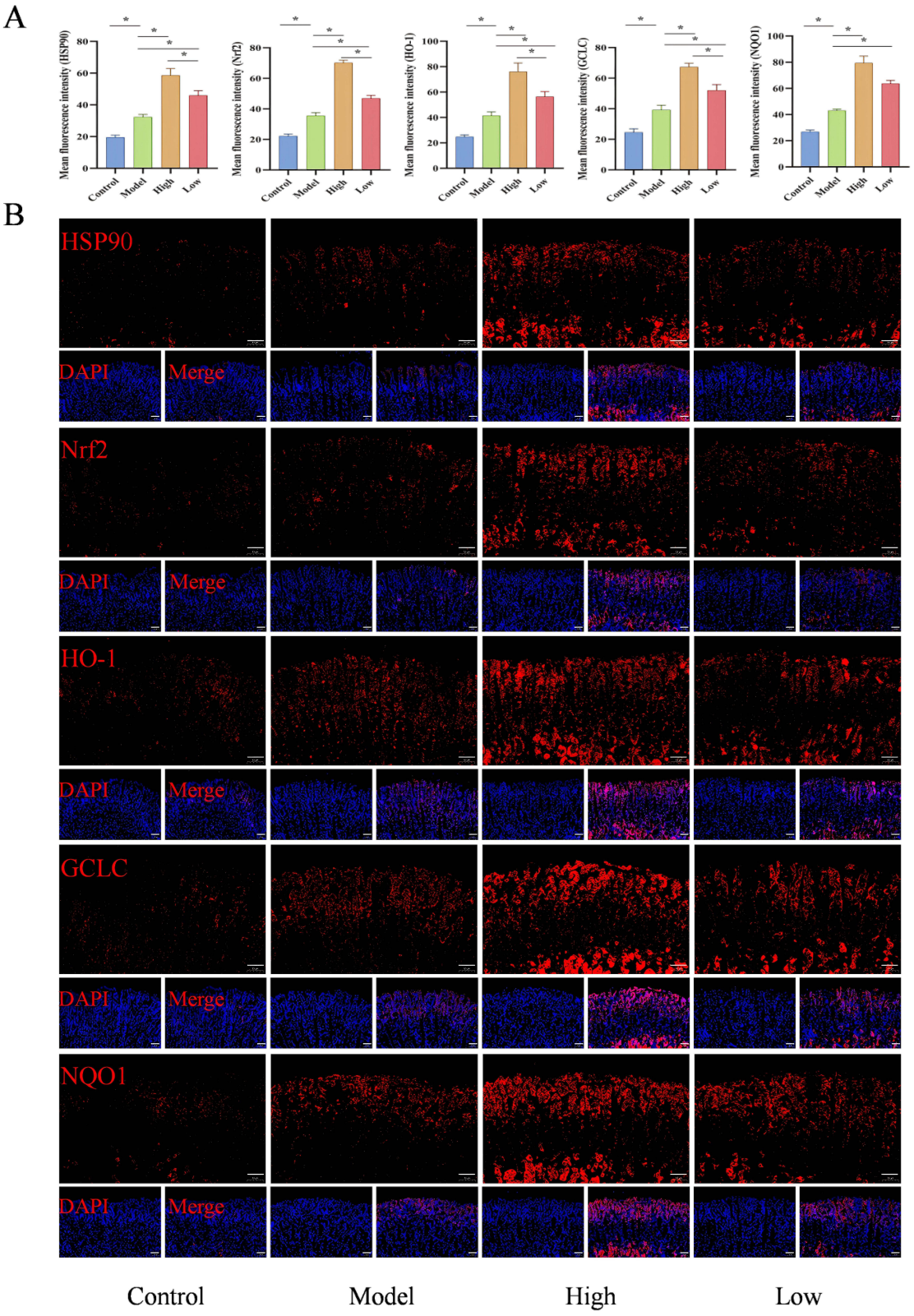

Figure 6 Effects of D-Mannose on the Protein Expression of Key Molecules in the HSP90/Nrf2/HO-1 Pathway. (**A** and **B**) Immunofluorescence detection of HSP90, Nrf2, HO-1, NQO1, and GCLC protein expression and quantitative analysis (n=3). Brightness and contrast adjustments were applied uniformly using Case Viewer 2.4 (**B**). Data are presented as mean±SD and were analyzed by one-way ANOVA followed by LSD/Tamhane's T2 post hoc test. *means $P < 0.05$.

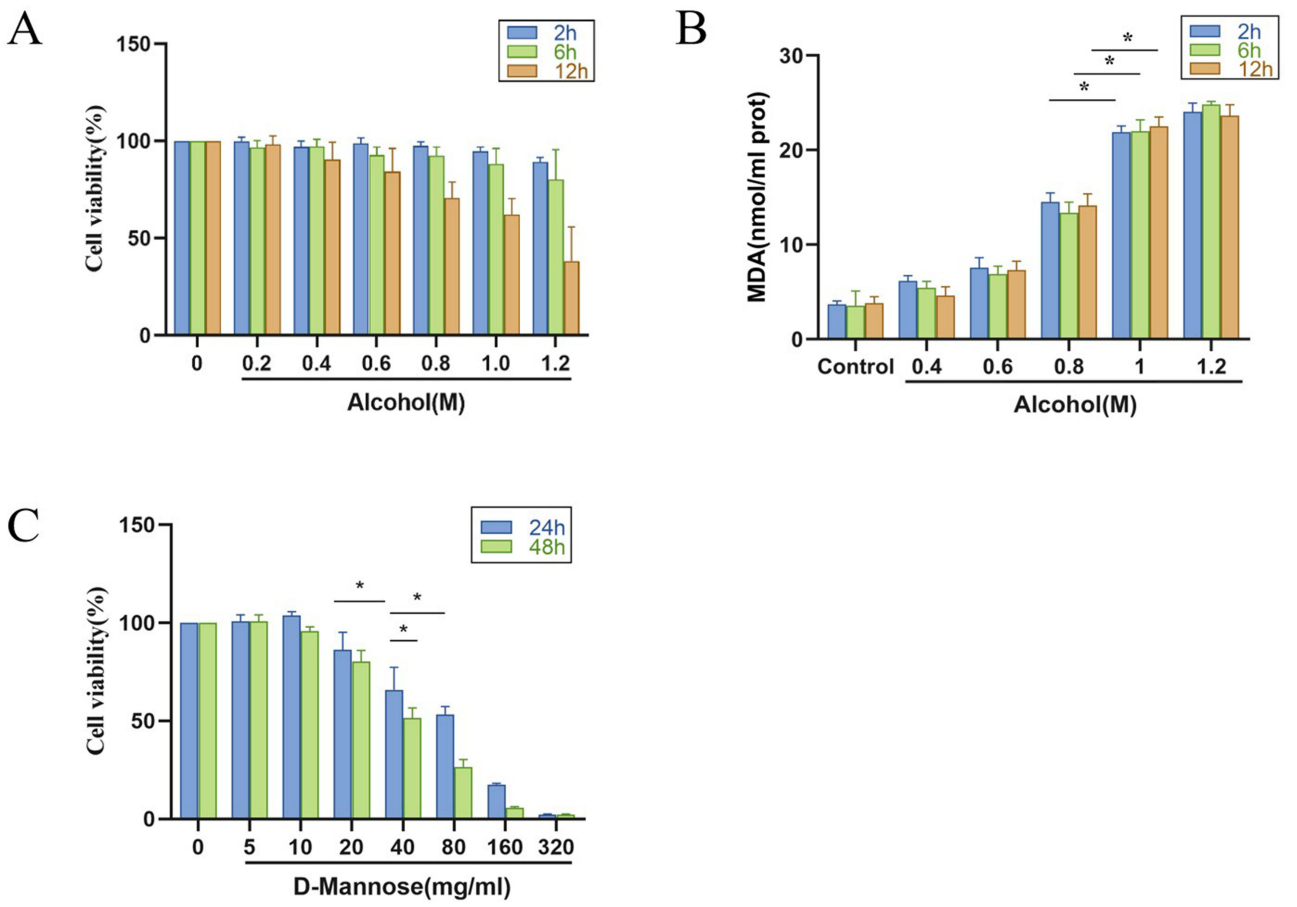

Figure 7 Cytotoxicity Evaluation of Different Concentrations of the Compounds. (**A**) Cell inhibition rate of anhydrous ethanol (n=6); (**B**) MDA content in GES-1 cells detected by biochemical assay kits (n=6); (**C**) Cytotoxicity evaluation of D-mannose (n=6). Data are presented as mean±SD and were analyzed by one-way ANOVA followed by LSD/Tamhane's T2 post hoc test. *means $P < 0.05$.

demonstrate the pivotal role of HSP90 in mediating D-mannose's protective mechanisms against oxidative cellular injury. Inhibition of HSP90 significantly attenuates the protective effects of D-mannose.

Discussion

GU is a common and recurrent gastrointestinal disorder that affects millions of individuals annually.[24] The development of GU is influenced by various factors, including physical factors (excessive alcohol consumption), chemical factors (long-term use of NSAIDs), biological factors (*Helicobacter Pylori* infection), and other factors such as prolonged mental stress and anxiety. The interplay of these elements destabilizes the equilibrium between defensive gastric mucosal mechanisms (including prostaglandins, protective mucus, and cellular renewal processes) and harmful physiological agents (such as acidic secretions and proteolytic enzymes), ultimately compromising the gastric epithelial defense system and inducing mucosal lesions.[25] Among these, excessive alcohol consumption is considered a critical factor in triggering ulcerative damage to the gastric mucosa.[26] Basic research has demonstrated that ethanol stimulation induces functional and morphological changes in the gastric mucosa of experimental animals, including abnormal mucus secretion, scattered hemorrhagic spots, and necrotic lesions in gastric tissues. These changes are remarkably similar to ulcerative damage observed in human gastric tissues.[27] Oxidative stress-induced injury is regarded as a key pathological mechanism underlying alcohol-induced damage to gastric tissues.[28] In this study, absolute ethanol was used to induce ulcerative damage to the gastric tissues of mice. Our findings revealed that, compared to Control mice, the Model group exhibited visibly apparent gastric mucosal bleeding and linear hemorrhagic streaks, accompanied by a significant increase in the

https://doi.org/10.2147/DDDT.S525021

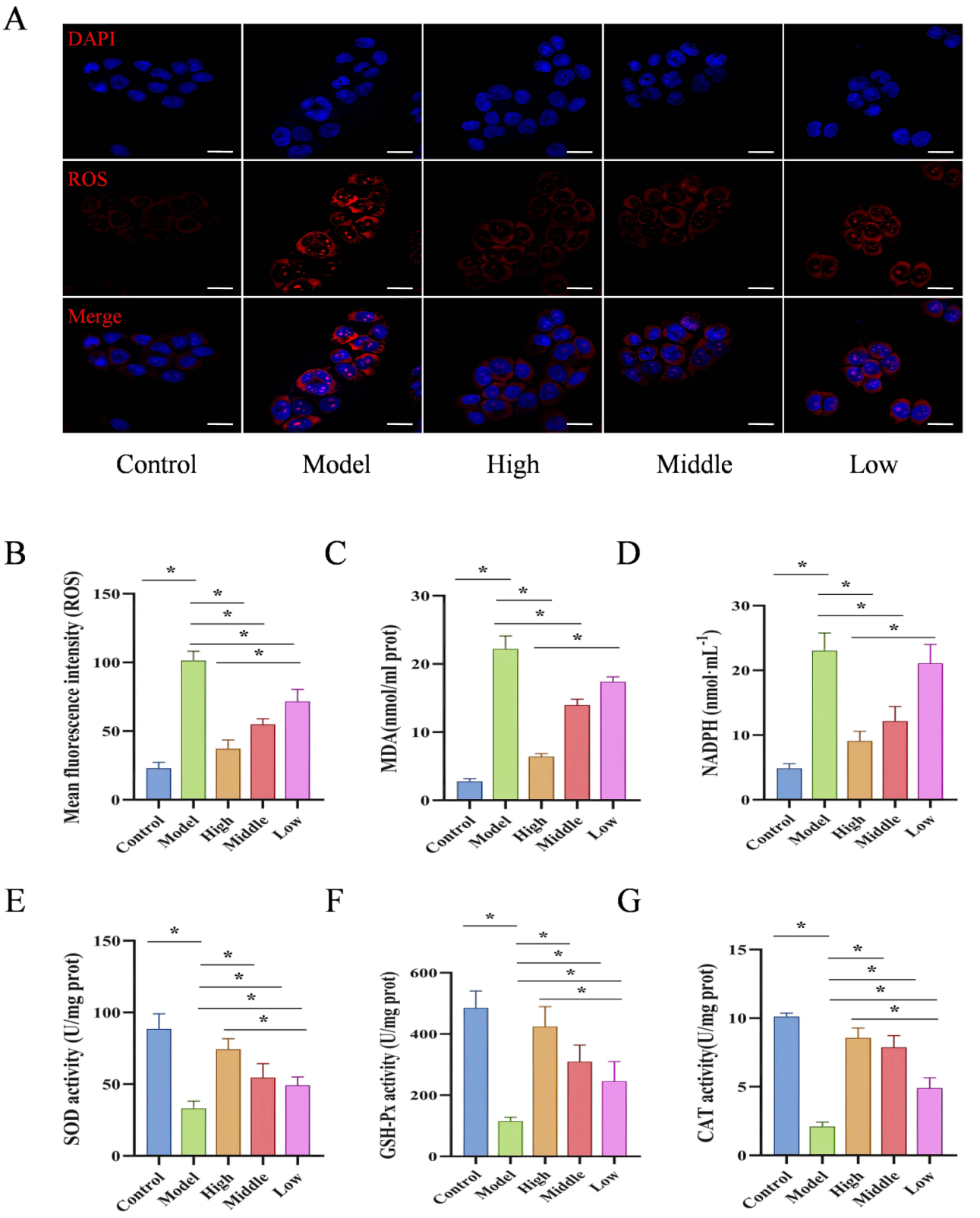

Figure 8 D-Mannose Alleviates Ethanol-Induced Oxidative Damage in GES-1 Cells. (**A** and **B**) Immunofluorescence analysis of ROS expression and quantitative ROS analysis (20 μm; n=3); (**C–G**) Biochemical assay kits for detecting MDA, NADPH, SOD, GSH-Px, and CAT levels (n=3). Brightness and contrast adjustments were applied uniformly using Case Viewer 2.4 (**A**). Data are presented as mean±SD and were analyzed by one-way ANOVA followed by LSD/Tamhane's T2 post hoc test. *means $P < 0.05$.

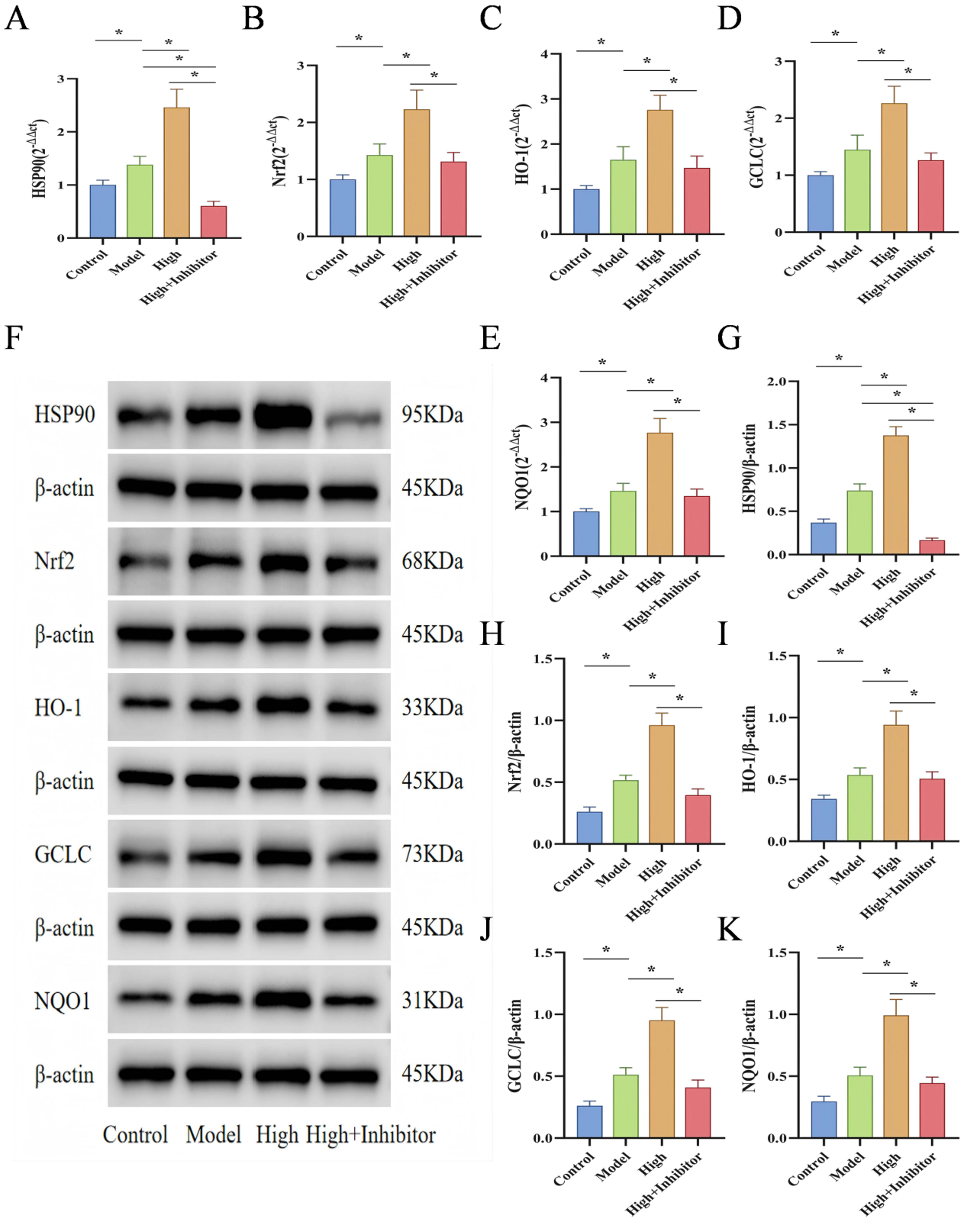

Figure 9 The Effect of HSP90 Inhibition on Gene and Protein Expression of Key Molecules in the HSP90/Nrf2/HO-1 Signaling Pathway. (**A–E**) RT-qPCR analysis of mRNA levels of *HSP90, Nrf2, HO-1, NQO1,* and *GCLC* in GES-1 cells (n=3); (**F–K**) Western blot analysis of protein expression and quantitative analysis of HSP90, Nrf2, HO-1, NQO1, and GCLC in GES-1 cells (n=3). Brightness and contrast adjustments were applied uniformly using Image J 1.42q (**F**). Data are presented as mean±SD and were analyzed by one-way ANOVA followed by LSD/Tamhane's T2 post hoc test. *means $P < 0.05$.

https://doi.org/10.2147/DDDT.S525021

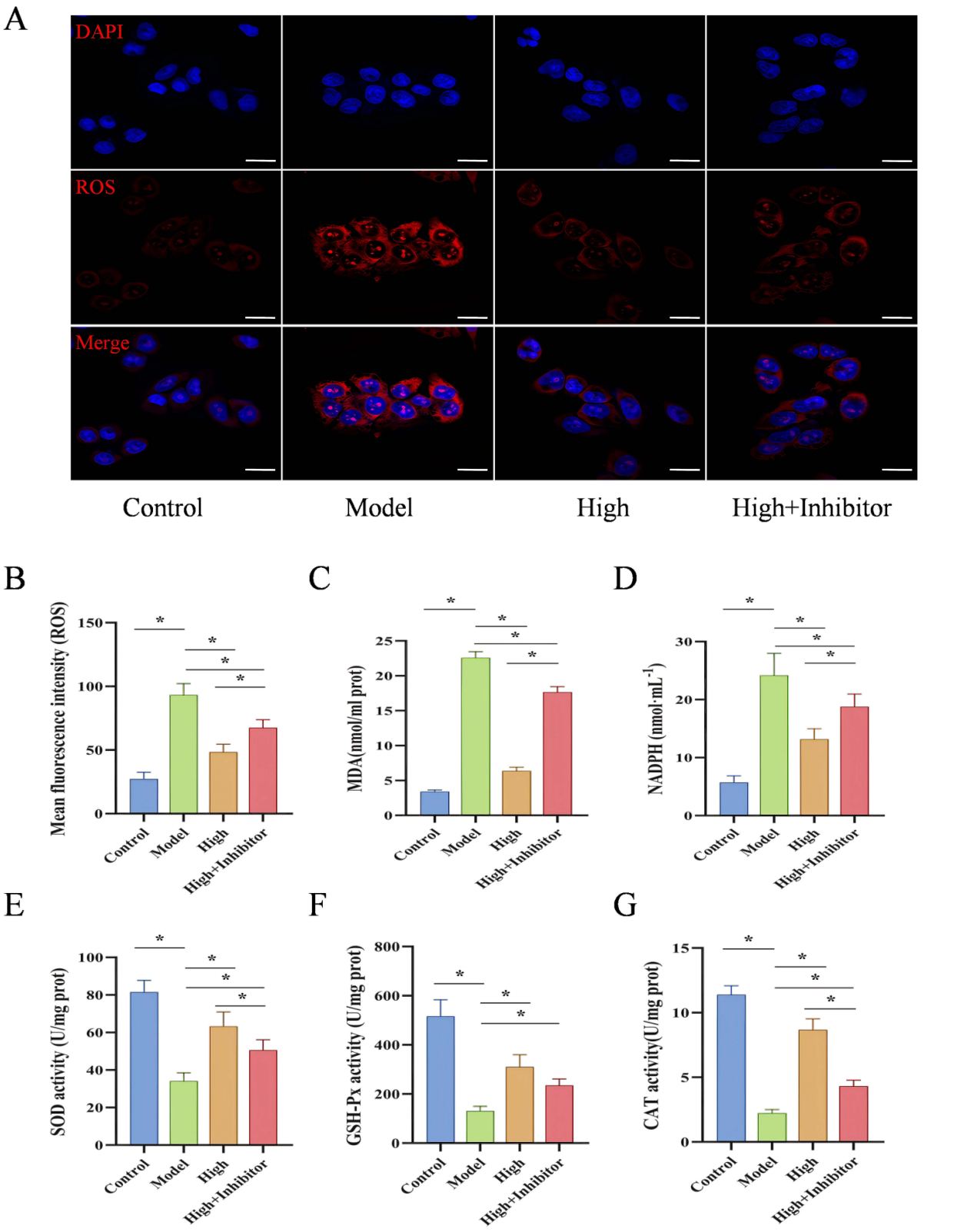

Figure 10 The HSP90/Nrf2/HO-1 Pathway as the Key Mechanism for D-Mannose in Reducing Oxidative Damage in GES-1 Cells. (**A** and **B**) Immunofluorescence analysis of ROS expression and quantitative ROS analysis (20 μm; n=3); (**C–G**) Biochemical assay kits for detecting the levels of MDA, NADPH, SOD, GSH-Px, and CAT (n=3). Brightness and contrast adjustments were applied uniformly using Case Viewer 2.4 (**A**). Data are presented as mean±SD and were analyzed by one-way ANOVA followed by LSD/Tamhane's T2 post hoc test. *means $P < 0.05$.

ulcer index. Histologically, the gastric tissues in the Model group exhibited epithelial cell necrosis and shedding, disorganized gastric gland structures, extensive hemorrhagic damage, inflammatory cell infiltration, and reduced secretion of mucin on the surface of the gastric mucosa. Observations under scanning electron microscopy further revealed severe damage to the gastric epithelial cells and disruption of the gastric pit structures, indicating that absolute ethanol successfully induced ulcerative damage in the gastric tissues of mice. Additionally, we found that the levels of ROS and the lipid peroxidation product MDA were significantly elevated in gastric tissues, while the activities of antioxidant enzymes, including SOD, GSH-Px, and CAT, were significantly reduced. These findings confirmed that absolute ethanol induced severe oxidative stress injury in the gastric tissues of mice, consistent with results from previous studies.[29]

D-mannose is a monosaccharide widely distributed in nature. Modern pharmacological studies have demonstrated that D-mannose possesses significant antioxidant potential. Shaker et al found that D-mannose reduces the production of MDA, enhances GSH activity, and alleviates thioacetamide-induced liver fibrosis.[19] Similarly, Zhou et al reported that D-mannose improves chondrocyte ferroptosis during cartilage degeneration in osteoarthritis by reducing excessive accumulation of ROS and MDA and enhancing the activities of SOD and GSH.[7] Our study employed different concentrations of D-mannose to treat mice with ethanol-induced gastric injury. The results indicated that, compared to the Model group, D-mannose ameliorated gastric tissue damage in a dose-dependent manner, with the high-dose group showing significantly superior therapeutic effects compared to the low-dose group. Furthermore, D-mannose significantly reduced the levels of ROS, MDA, and NADPH while increasing the activities of SOD, GSH-Px, and CAT. These findings demonstrate that D-mannose can markedly enhance the antioxidant capacity of gastric tissues and counteract oxidative stress-induced damage, with the high-dose regimen producing the most pronounced protective effects.

Network pharmacology effectively constructs a "component-protein/gene-disease" network,[30] while molecular docking facilitates the study of interactions between molecules (eg, ligands and receptors) and predicts their binding patterns and affinities.[31] Through a sophisticated computational strategy integrating network-based pharmacological prediction and molecular interaction modeling, we systematically investigated the critical molecular targets potentially involved in D-mannose's therapeutic response for GU management. Network pharmacology analysis identified four core target molecules: HSP90AA1, PRKCA, ESR2, and STAT3. Through rigorous in silico docking simulations, the D-mannose molecular ligand exhibited the most significant binding affinity towards the HSP90 molecular target, suggesting that HSP90 may be the critical target molecule through which D-mannose ameliorates ethanol-induced gastric tissue ulceration. HSP90 is one of the key members of the heat shock protein family. Under conditions of cellular distress and structural tissue impairment, the mechanism demonstrates the capability of initiation, and it is considered an additional factor involved in gastric defense mechanisms at the intracellular level. Most of its target proteins are protein kinases or transcription factors, which actively participate in the biological processes of gastric ulcer healing.[32] Existing studies have confirmed that the occurrence of gastric ulcers is accompanied by abnormally activated expression of HSP90.[33] The experimental results further substantiated these observations: relative to baseline conditions, absolute ethanol treatment induced a statistically significant upregulation of HSP90 gene and protein levels within gastric tissue specimens.

Oxidative stress refers to an imbalance caused by the excessive production of oxidants exceeding the antioxidant capacity of the cellular defense system.[34] Extensive scientific research suggests that oxidative mechanisms serve as a fundamental driving force underlying the initiation and evolution of ethanol-associated GU pathology.[35] Ethanol depletes mucus and bicarbonate, leading to hypoxia in the gastric mucosa and the spread of inflammatory cascades, which ultimately result in cell necrosis and excessive ROS production.[36] ROS, either directly or indirectly, impair the physiological functions of intracellular macromolecules such as proteins, lipids, and nucleic acids. This damage disrupts the gastric mucosal barrier and hinders mucosal repair, thereby causing ulcerative damage to gastric tissues.[37] The Nrf2/HO-1 signaling cascade emerges as a critical molecular sentinel, adeptly perceiving both external and internal oxidative challenges while implementing cellular protection through targeted transcriptional induction of protective genomic elements.[38] Interestingly, the molecular chaperone HSP90, as an important auxiliary factor of Nrf2, has been shown to genetically and physically interact with Nrf2 in yeast models.[39] Moreover, Wang et al found that HSP90 and Nrf2 jointly participate in systemic cytoprotective stress responses in non-neuronal cells.[40] We conducted a detailed assessment of HSP90 and key molecular constituents of the Nrf2/HO-1 signaling mechanism, examining both transcriptional and translational expression levels within gastric tissue samples. Comparative analysis revealed that, relative to Control subjects, the Model group demonstrated statistically significant upregulation of

mRNA and protein expression for *HSP90, Nrf2, HO-1,* and *NQO1* within gastric tissue specimens. However, compared to the Model group, the mRNA and protein levels of these molecules were further elevated in the gastric tissues of mice pretreated with D-mannose, with the high-dose group demonstrating significantly greater upregulation than the low-dose group.

The gastric epithelial cells form a mechanical barrier through tight junctions between the apical membrane and the lateral membranes of adjacent cells, effectively preventing the diffusion of H^+ from the gastric lumen into the epithelial cells. Additionally, the gastric epithelial cells secrete mucus, which forms a protective layer on the mucosal surface. This mucus layer combines with $HCO3^-$ in the gastric lumen to create a mucus-bicarbonate barrier, effectively resisting the damage caused by gastric acid and pepsin to the gastric mucosa.[41] GES-1 cells, a commonly used gastric epithelial cell line, exhibit fundamental characteristics and functions of normal human gastric mucosal epithelial cells. These cells have been widely used for evaluating the gastroprotective activity of natural products in vitro.[42] Current studies have shown that alcohol-induced gastric ulcer damage is closely associated with excessive oxidative stress in gastric epithelial cells.[43] In our research, ethanol-treated GES-1 cells were employed to investigate the oxidative stress damage induced by ethanol. Experimental evidence conclusively revealed that ethanol exposure triggered substantial oxidative stress-mediated cellular damage mechanisms. In contrast to normal cellular parameters, ethanol treatment dramatically reduced GES-1 cell survival potential, while simultaneously triggering substantial augmentations in intracellular oxidative stress indicators (ROS, MDA, and NADPH). Meanwhile, the activities of SOD, GSH-Px, and CAT were noticeably decreased. In the subsequent experimental phase, GES-1 cells underwent systematic intervention with varying D-mannose concentration gradients. The results showed that D-mannose significantly enhanced the antioxidant capacity of GES-1 cells and alleviated ethanol-induced oxidative stress damage, with the most pronounced effect observed in the high-dose group (40 mg/mL). Our previous animal experiments revealed that D-mannose alleviated ethanol-induced oxidative damage by activating the HSP90/Nrf2/HO-1 signaling pathway. To further validate this mechanism, we used an HSP90 inhibitor to intervene in GES-1 cells. Compared with the D-mannose treatment group, the combined group exhibited aggravated oxidative damage, suggesting that the HSP90/Nrf2/HO-1 signaling pathway plays a critical role in the protective effect of D-mannose against oxidative damage in GES-1 cells.

Our animal experiments confirmed that D-mannose, by activating the HSP90/Nrf2/HO-1 signaling pathway, enhances the activities of antioxidant enzymes SOD, GSH-Px, and CAT, reduces the generation of oxygen radical ROS and lipid peroxidation product MDA, thereby improving the antioxidant capacity of the organism and gastric tissues. This results in the alleviation of ulcerative damage to gastric tissues induced by absolute ethanol. Similarly, the cell experiments demonstrated that D-mannose activates the gene and protein expression of key molecules in the HSP90/Nrf2/HO-1 pathway, thereby counteracting ethanol-induced oxidative stress damage in gastric epithelial cells.

Conclusion

In summary, our research findings demonstrate that D-mannose possesses significant gastroprotective activity, primarily through enhancing the antioxidant capacity of the body and gastric tissues by activating the HSP90/Nrf2/HO-1 signaling pathway, thereby counteracting oxidative damage induced by absolute ethanol.

Limitations and Future Perspectives

However, this study has certain limitations. First, the etiology of GU is diverse and its pathogenesis is complex. This study evaluated only the protective effect of D-mannose on ethanol-induced gastric ulcers. Other factors such as abuse of NSAIDs, *Helicobacter Pylori* infection, and prolonged mental stress can also lead to gastric mucosal damage. Therefore, further research is needed to establish other types of gastric ulcer models to achieve a comprehensive evaluation of D-mannose's effects. Second, Through network pharmacology and molecular docking, this study identified HSP90 as a key target. However, the network pharmacology analysis lacked associated enrichment studies. Furthermore, while the Nrf2/HO-1 pathway was selected for subsequent investigation, the regulatory relationships between its upstream and downstream components were insufficiently explored. Therefore, additional target validation experiments are required to improve the experimental comprehensiveness. Third, some experiments were limited by a small sample size ($n < 5$). Due to the small volume of mouse gastric tissue samples, it was not feasible to subject the same sample to multiple different treatments. Therefore, under the limited conditions, we rationally allocated the tissue samples, resulting in a sample size of $n = 3$ for some experiments. Despite this, we ensured the reliability of the experimental results through the following measures: On the one

hand, we observed the macroscopic morphology and pathological damage of the gastric tissues of each group of mice, and conducted quantitative analysis of ulcer area and pathological scoring, which fully demonstrated the homogeneity among the enrolled animals. On the other hand, based on the characteristics of the experimental data, we selected appropriate statistical analysis methods. For data that were not normally distributed and had a small sample size ($n < 5$), permutation tests were used for inter-group comparisons. In future studies, we plan to increase the sample size ($n > 5$) and further optimize the experimental design to enhance the robustness and reproducibility of the results. Four, This study has so far only combined D-mannose with an HSP90 inhibitor in vitro, and their interaction has not yet been validated through more comprehensive in vivo mechanistic investigations. Further combined administration of an HSP90 inhibitor in mouse models would expectedly significantly strengthen the causal relationship between HSP90 activation and the gastroprotective effects of D-mannose. Therefore, we plan to conduct in-depth related experiments in follow-up studies.

Data Sharing Statement

The data presented in this study are available from the corresponding author on reasonable request.

Author Contributions

All authors made a significant contribution to the work reported, whether that is in the conception, study design, execution, acquisition of data, analysis and interpretation, or in all these areas; took part in drafting, revising or critically reviewing the article; gave final approval of the version to be published; have agreed on the journal to which the article has been submitted; and agree to be accountable for all aspects of the work.

Funding

This work was supported by the open project of Gansu Research Center of Traditional Chinese Medicine (No. ZYFY-2020-001).

Disclosure

The authors report no conflicts of interest in this work. This paper is available on ssrn as a preprint https://papers.ssrn.com/sol3/papers.cfm?abstract_id=5124695

References

1. Tarnawski AS, Ahluwalia A. The critical role of growth factors in gastric ulcer healing: the cellular and molecular mechanisms and potential clinical implications. *Cells*. 2021;10(8):1964. doi:10.3390/cells10081964
2. Feng L, Bao T, Bai L, et al. Mongolian medicine formulae Ruda-6 alleviates indomethacin-induced gastric ulcer by regulating gut microbiome and serum metabolomics in rats. *J Ethnopharmacol*. 2023;314:116545. doi:10.1016/j.jep.2023.116545
3. Shams SGE, Eissa RG. Amelioration of ethanol-induced gastric ulcer in rats by quercetin: implication of Nrf2/HO1 and HMGB1/TLR4/NF-κB pathways. *Heliyon*. 2022;8(10):e11159. doi:10.1016/j.heliyon.2022.e11159
4. Xie C, Liu L, Zhu S, Wei M. Effectiveness and safety of Chinese medicine combined with omeprazole in the treatment of gastric ulcer: a protocol for systematic review and meta-analysis. *Medicine*. 2021;100(17):e25744. doi:10.1097/md.0000000000025744
5. Freedberg DE, Kim LS, Yang YX. The Risks and benefits of long-term use of proton pump inhibitors: expert review and best practice advice from the American gastroenterological association. *Gastroenterology*. 2017;152(4):706–715. doi:10.1053/j.gastro.2017.01.031
6. Chen S, Wang K, Wang Q. Mannose: a promising player in clinical and biomedical applications. *Curr Drug Deliv*. 2024;21(11):1435–1444. doi:10.2174/0115672018275954231220101637
7. Zhou X, Zheng Y, Sun W, et al. D-mannose alleviates osteoarthritis progression by inhibiting chondrocyte ferroptosis in a HIF-2α-dependent manner. *Cell Prolif*. 2021;54(11):e13134. doi:10.1111/cpr.13134
8. Wang B, Zhang H, Chen L, et al. Extraction, purification, and determination of the gastroprotective activity of glucomannan from Bletilla striata. *Carbohydr Polym*. 2020;246:116620. doi:10.1016/j.carbpol.2020.116620
9. Jian TZ, Chen N, Li LX, et al. Effects of D-mannose and glucose on ulcerative colitis in mice. *J Shandong Univ*. 2022;60(03):24–28. in Chinese.
10. Luo M, Sun J, Li S, et al. Protective effect of Enterococcus faecium against ethanol-induced gastric injury via extracellular vesicles. *Microbiol Spectr*. 2024;12(4):e0389423. doi:10.1128/spectrum.03894-23
11. Luo JH, Zou WS, Li J, et al. Untargeted serum and liver metabolomics analyses reveal the gastroprotective effect of polysaccharide from Evodiae fructus on ethanol-induced gastric ulcer in mice. *Int J Biol Macromol*. 2023;232:123481. doi:10.1016/j.ijbiomac.2023.123481
12. Gong H, Zhao N, Zhu C, et al. Treatment of gastric ulcer, traditional Chinese medicine may be a better choice. *J Ethnopharmacol*. 2024;324:117793. doi:10.1016/j.jep.2024.117793
13. Ren S, Wei Y, Niu M, et al. Mechanism of rutaecarpine on ethanol-induced acute gastric ulcer using integrated metabolomics and network pharmacology. *Biomed Pharmacother*. 2021;138:111490. doi:10.1016/j.biopha.2021.111490

14. Zhou C, Chen J, Liu K, et al. Isoalantolactone protects against ethanol-induced gastric ulcer via alleviating inflammation through regulation of PI3K-Akt signaling pathway and Th17 cell differentiation. *Biomed Pharmacother*. 2023;160:114315. doi:10.1016/j.biopha.2023.114315
15. Hu Y, Liu T, Zheng G, et al. Mechanism exploration of 6-Gingerol in the treatment of atherosclerosis based on network pharmacology, molecular docking and experimental validation. *Phytomedicine*. 2023;115:154835. doi:10.1016/j.phymed.2023.154835
16. Deng Q, Chen W, Deng B, et al. Based on network pharmacology, molecular docking and experimental verification to reveal the mechanism of Andrographis paniculata against solar dermatitis. *Phytomedicine*. 2024;135:156025. doi:10.1016/j.phymed.2024.156025
17. Lv Y, Li J, Li Y, et al. Unveiling the potential mechanisms of Amomi fructus against gastric ulcers via integrating network pharmacology and in vivo experiments. *J Ethnopharmacol*. 2024;319(Pt 2):117179. doi:10.1016/j.jep.2023.117179
18. Guo H, Xu Z, Zhu L, et al. Standardized aqueous extract of Abutilon theophrasti Medic. ameliorates oxidative stress and inflammatory responses against hydrochloric acid/ethanol-induced gastric ulcer in rats. *Front Pharmacol*. 2025;16:1599810. doi:10.3389/fphar.2025.1599810
19. Shaker ME, Eisa NH, Elgaml A, et al. Ingestion of mannose ameliorates thioacetamide-induced intrahepatic oxidative stress, inflammation and fibrosis in rats. *Life Sci*. 2021;286:120040. doi:10.1016/j.lfs.2021.120040
20. Liu H, Chen Y, Hu Y, et al. Protective effects of an alcoholic extract of Kaempferia galanga L. rhizome on ethanol-induced gastric ulcer in mice. *J Ethnopharmacol*. 2024;325:117845. doi:10.1016/j.jep.2024.117845
21. Huang H, Hou Y, Chen L, et al. Multifunctional gallic acid self-assembled hydrogel for alleviation of ethanol-induced acute gastric injury. *Int J Pharm*. 2023;645:123372. doi:10.1016/j.ijpharm.2023.123372
22. Yoo JH, Park EJ, Kim SH, Lee HJ. Gastroprotective effects of fermented lotus root against ethanol/HCl-induced gastric mucosal acute toxicity in rats. *Nutrients*. 2020;12(3):808. doi:10.3390/nu12030808
23. Ortaç D, Cemek M, Karaca T, et al. In vivo anti-ulcerogenic effect of okra (Abelmoschus esculentus) on ethanol-induced acute gastric mucosal lesions. *Pharm Biol*. 2018;56(1):165–175. doi:10.1080/13880209.2018.1442481
24. Mai Y, Xu S, Shen R, et al. Gastroprotective effects of water extract of domesticated Amauroderma rugosum against several gastric ulcer models in rats. *Pharm Biol*. 2022;60(1):600–608. doi:10.1080/13880209.2022.2047210
25. Feng L, L A, Li H, et al. Pharmacological mechanism of aucklandiae radix against gastric ulcer based on network pharmacology and in vivo experiment. *Medicina*. 2023;59(4):666. doi:10.3390/medicina59040666
26. Zhai C, Lu F, Du X, et al. Green carbon dots derived from Atractylodes macrocephala: a potential nanodrug for treating alcoholic gastric ulcer. *Colloids Surf B Biointerfaces*. 2023;230:113492. doi:10.1016/j.colsurfb.2023.113492
27. Zhou D, Yang Q, Tian T, et al. Gastroprotective effect of gallic acid against ethanol-induced gastric ulcer in rats: involvement of the Nrf2/HO-1 signaling and anti-apoptosis role. *Biomed Pharmacother*. 2020;126:110075. doi:10.1016/j.biopha.2020.110075
28. Sanpinit S, Chonsut P, Punsawad C, et al. Gastroprotective and antioxidative effects of the traditional Thai polyherbal formula phy-blica-d against ethanol-induced gastric ulcers in rats. *Nutrients*. 2021;14(1):172. doi:10.3390/nu14010172
29. Zhao Z, Wei G, Wang L, et al. Pretreatment with Dan-Shen-Yin granules alleviates ethanol-induced gastric mucosal damage in rats by inhibiting oxidative stress and apoptosis via Akt/Nrf2 signaling pathway. *Phytomedicine*. 2024;132:155866. doi:10.1016/j.phymed.2024.155866
30. Zhou Z, Chen B, Chen S, et al. Applications of network pharmacology in traditional Chinese medicine research. *Evid Based Complement Alternat Med*. 2020;2020:1646905. doi:10.1155/2020/1646905
31. Tong X, Xu S, Zhai D. Multiple mechanisms of shenqi pill in treating nonalcoholic fatty liver disease based on network pharmacology and molecular docking. *Evid Based Complement Alternat Med*. 2022;2022:2384140. doi:10.1155/2022/2384140
32. Choi SR, Lee SA, Kim YJ, et al. Role of heat shock proteins in gastric inflammation and ulcer healing. *J Physiol Pharmacol*. 2009;60(Suppl 7):5–17.
33. Guo H, Chen B, Yan Z, et al. Metabolites profiling and pharmacokinetics of troxipide and its pharmacodynamics in rats with gastric ulcer. *Sci Rep*. 2020;10(1):13619. doi:10.1038/s41598-020-70312-7
34. Wu H, Kong Y, Zhao W, et al. Measurement of cellular MDA content through MTBE-extraction based TBA assay by eliminating cellular interferences. *J Pharm Biomed Anal*. 2024;248:116332. doi:10.1016/j.jpba.2024.116332
35. Badr AM, El-Orabi NF, Mahran YF, et al. In vivo and In silico evidence of the protective properties of carvacrol against experimentally-induced gastric ulcer: implication of antioxidant, anti-inflammatory, and antiapoptotic mechanisms. *Chem Biol Interact*. 2023;382:110649. doi:10.1016/j.cbi.2023.110649
36. Wu T, Zhang H, Jin Y, et al. The active components and potential mechanisms of Wuji Wan in the treatment of ethanol-induced gastric ulcer: an integrated metabolomics, network pharmacology and experimental validation. *J Ethnopharmacol*. 2024;326:117901. doi:10.1016/j.jep.2024.117901
37. Hossen MA, Reza A, Ahmed AMA, et al. Pretreatment of Blumea lacera leaves ameliorate acute ulcer and oxidative stress in ethanol-induced long-evan rat: a combined experimental and chemico-biological interaction. *Biomed Pharmacother*. 2021;135:111211. doi:10.1016/j.biopha.2020.111211
38. Liu Y, Wang S, Jin G, et al. Network pharmacology-based study on the mechanism of ShenKang injection in diabetic kidney disease through Keap1/Nrf2/Ho-1 signaling pathway. *Phytomedicine*. 2023;118:154915. doi:10.1016/j.phymed.2023.154915
39. Ngo V, Brickenden A, Liu H, et al. Duennwald ML. A novel yeast model detects Nrf2 and Keap1 interactions with Hsp90. *Dis Model Mech*. 2022;15(4):dmm049235. doi:10.1242/dmm.049258
40. Wang J, Wang J, Li Y, et al. Organic selenium alleviates ammonia-mediated abnormal autophagy by regulating inflammatory pathways and the Keap1/Nrf2 axis in the hypothalamus of finishing pigs. *Biol Trace Elem Res*. 2023;201(8):3812–3824. doi:10.1007/s12011-022-03452-8
41. Ye HY, Shang ZZ, Zhang FY, et al. Dendrobium huoshanense stem polysaccharide ameliorates alcohol-induced gastric ulcer in rats through Nrf2-mediated strengthening of gastric mucosal barrier. *Int J Biol Macromol*. 2023;236:124001. doi:10.1016/j.ijbiomac.2023.124001
42. Zhang Y, Liang J, Jiang H, et al. Protective effect of sterols extracted from Lotus plumule on ethanol-induced injury in GES-1 cells in vitro. *Food Funct*. 2021;12(24):12659–12670. doi:10.1039/d1fo02684d
43. Duan Z, Yu S, Wang S, et al. Protective effects of piperine on ethanol-induced gastric mucosa injury by oxidative stress inhibition. *Nutrients*. 2022;14(22):4744. doi:10.3390/nu1422474